SUPPLEMENTARY INFORMATION

Pelagic photoferrotrophy and Iron cycling in a modern ferruginous basin

Marc Llirós[1,2,*,†], Tamara García–Armisen[3], François Darchambeau[4], Cédric Morana[5], Xavier Triadó–Margarit[6,7], Özgül Inceoğlu[3], Carles M Borrego[7,8], Steven Bouillon[5], Pierre Servais[3], Alberto V Borges[4], Jean–Pierre Descy[1], Don E Canfield[9] & Sean A Crowe[9,10,*].

[†]Present address: Institute des Sciences de la Vie, Université Catholique de Louvain, Place Croix du Sud 4/5, B-1348 Louvain-La-Neuve, Belgium.

[*]Authors to whom correspondence should be addressed.

15 **SUPPLEMENTARY METHODS**

16 *Site description and sampling*

17 Kabuno Bay (KB, 1.58º–1.70º S, 29.01º–29.09º E; DR Congo) is a sub-basin of Lake
18 Kivu located in the East African Rift system. KB has a surface area of 48 km^2 and a
19 maximum depth of 120 m and is permanently stratified. Many physical and chemical
20 characteristics of the basin are related to its isolation from the main lake due to its 150
21 m wide and 10 m deep connection[1]. Further details on KB and Lake Kivu are published
22 elsewhere[2-11]. Water samples were collected at different depths during two sampling
23 campaigns conducted during 2012 covering both the rainy (RS, February) and the dry
24 (DS, October) seasons using either a battery-driven peristaltic pump connected to a
25 weighted-double conical intake through plastic tubing (for those depths corresponding
26 to the oxic-anoxic transition zone) or a 5-l vertical Niskin bottle (Hydro-Bios; for the
27 rest of the depths). Water samples were processed immediately for chemical analyses or
28 subsequently stored in 4-l plastic containers at 4°C for further processing for molecular
29 microbiology.

30 *Physico-chemical analyses*

31 Vertical depth profiles of temperature, conductivity, pH, and oxygen were measured *in*
32 *situ* with either Hydrolab DS5 (OTT Hydromet, Germany) or a Sea&Sun CTD90 (Sea
33 and Sun Technology, Germany) multiparametric probes. Photosynthetically Active
34 Radiation (PAR) was measured by means of a Li-Cor LI-193SA spherical quantum
35 sensor apparatus (Lincoln, NE, USA). Fe speciation was measured by ferrozine
36 method[12]. CH_4 concentrations in the collected water samples were determined as
37 previously described[9,13] via the headspace equilibration technique and gas
38 chromatography[14].

39 Water samples for NOx (*i.e.*, NO_3^- and NO_2^-) analyses were directly passed through
40 0.22 µm pore size cellulose acetate syringe filters and stored frozen until analyses with
41 no preservative. NO_2^- concentrations were determined following the sulphanilamide
42 coloration method[15], whereas NO_3^- concentrations were measured after vanadium
43 reduction to nitrite and further quantified as previously described[15,16]. Samples for
44 Hydrogen (H_2) determinations were conducted by headspace equilibration
45 technique[17,18]. Furthermore, acetate (CH_3COO^-) concentrations were measured from

46 frozen water samples collected during the DS sampling campaign by Ion
47 Chromatography using a Dionex Instrument as described here[19].

48 Samples for the determination of the stable isotope composition ($\delta^{13}C$) of dissolved
49 inorganic carbon (DIC) were collected by gently overfilling 12 ml glass vial (Labco
50 Exetainer) preserved with 20 µl of saturated $HgCl_2$ (final conc., 0.45 mM). For the
51 analysis of $\delta^{13}C$-DIC, a 2 ml helium headspace was created and 100 µl of H_3PO_4 (99%)
52 was added into each vial to convert all DIC species into CO_2. After overnight
53 equilibration, a variable volume of the headspace was injected into an elemental
54 analyser coupled to an isotope ratio mass spectrometer (EA-IRMS; Thermo FlashHT
55 with Thermo DeltaV Advantage). Calibration of $\delta^{13}C$-DIC measurements was
56 performed with certified reference materials (LSVEC and either NBS-19 or IAEA-CO-
57 1). Samples for the determination of the concentration and the stable isotope
58 composition ($\delta^{13}C$) of particulate organic C (POC) were obtained by filtering a known
59 volume of water on pre-combusted (overnight at 450ºC) 0.3 µm pore-size 25 mm
60 diameter glass fiber filters (Advantec GF-75) and kept frozen (–20ºC) until processing.
61 Filters were decarbonated with HCl fumes for 4h, dried, packed in silver cups and
62 analysed on an EA–IRMS (Thermo FlashHT with Thermo DeltaV Advantage).
63 Acetanilide ($\delta^{13}C$ = –27.65‰ ± 0.05) and Leucine ($\delta^{13}C$ = –13.47‰ ± 0.07) were used
64 as standards, and were calibrated in-house against certified standards (IAEA-CH-6).
65 Relative standard deviation for POC measurements was below 5%, and analytical
66 uncertainty for (natural abundance) $\delta^{13}C$-POC measurements was typically better than
67 0.15‰.

68 *Pigment analyses*

69 Water samples for pigment analyses (2.0 to 3.0 l) were collected and subsequently
70 passed through 47 mm diameter Macherey-Nägel GF5 filters (Düren, Germany).
71 Chlorophyll (Chl)-related pigments were analysed by High Performance Liquid
72 Chromatography (HPLC) from 90% acetone (Fischer Chemical) extracts (10 ml final
73 volume) according to[20,21]. Identification and quantification of pigments were done
74 according to retention times and specific absorption spectra in the eluent solvents.
75 Calibration and Chl *a* quantification were undertaken by using commercial external
76 standards (DHI, Denmark). The complete separation and quantification of

77 bacteriochlorophyll (BChl) pigments and homologues was determined from the total
78 area of the corresponding peaks and using appropriate molar absorption coefficients[22,23].

79 *Total cell abundances*

80 Total cell abundances were quantified by flow cytometry as previously described[7].

81 *Simple isotope mass balance*

82 The contribution of *Chlorobium*-derived carbon to the POC pool (%$POC_{Chlorobium}$) at a
83 given depth (z) was estimated via an isotope mass balance approach, as:

84 %$POC_{Chlorobium}$ = (100 x $\delta^{13}C$-POC_z – 100 x $\delta^{13}C$-POC_{ML}) / ($\delta^{13}C$-*Chlorobium* – $\delta^{13}C$-
85 POC_{ML})

86 where $\delta^{13}C$-POC_z is the $\delta^{13}C$ signature of the POC at the depth z, $\delta^{13}C$-POC_{ML} (–27.5‰
87 ± 0.3, n = 3) is the $\delta^{13}C$ signature of the POC in the mixed layer, and $\delta^{13}C$-*Chlorobium*
88 is the theoretical $\delta^{13}C$ signature of the *Chlorobium*, estimated based on the isotope
89 fractionation factor for C fixation by *Chlorobioum* via the rTCA pathway (–12.2‰,[24])
90 and the measured $\delta^{13}C$-DIC in the chemocline (–5.3‰ ± 0.2, n = 5).

91 *Light and dark CO_2 fixation*

92 Photo- and chemoautotrophic bulk CO_2 fixation rates were quantified in 60 ml glass
93 serum bottles from selected depths covering the oxic-anoxic transition zone of KB
94 during both RS and DS. Serum bottles (eight per depth) were overflowed 3 times,
95 completely filled avoiding bubbles and then capped with butyl stoppers and crimp-
96 sealed with aluminium caps. The incubation set included clear (light) and dark
97 (aluminium foil covered) triplicate bottles. All samples were spiked with 1 ml of a ^{13}C-
98 DIC solution (99.8% $NaH^{13}CO_3$ dissolved in lake water; final concentration 1mM,
99 equivalent to less than 8% of total DIC stock) through the septa. Additionally, one
100 $HgCl_2$-killed bottle for each condition was incubated as a control without biological
101 activity. Each bottle was gently shaken and incubated for 24h at their corresponding
102 depths. After incubation, 40 ml sub-samples were passed through 0.3 µm pore-size
103 glass fiber filters (Advantec GF-75) to trace ^{13}C-DIC incorporation into the POC pool,
104 and 12 ml sub-samples were used to fill Exetainer tubes (LabCo) poisoned with 20 µl of
105 a saturated solution of $HgCl_2$ (final conc., 0.45 mM) to determine the exact ^{13}C-
106 enrichment in the DIC pool in every bottle. Measurement of the $\delta^{13}C$-DIC and $\delta^{13}C$-

107 POC were carried out as described above. CO_2 fixation rates (μmol l^{-1} d^{-1}) were
108 calculated as previously described[25] from dark and light bottles according to equations
109 (1) and (2):

110 (1) $DarkCO_2 = [POC_f \times (\%^{13}C\text{-}POC_f - \%^{13}C\text{-}POC_i)] \times [t \times (\%^{13}C\text{-}DIC - \%^{13}C\text{-}$
111 $POC_i)]^{-1}$

112 (2) $LightCO_2 = [(POC_f \times (\%^{13}C\text{-}POC_f - \%^{13}C\text{-}POC_i)) \times (t \times (\%^{13}C\text{-}DIC - \%^{13}C\text{-}$
113 $POC_i))^{-1}] - DarkCO_2$

114 where POC_f is the POC concentration at the end of the incubation, $\%^{13}C$-POC_i and
115 $\%^{13}C$-POC_f are the initial an final percentage of ^{13}C in POC, t is the incubation time and
116 $\%^{13}C$-DIC is the percentage of ^{13}C in DIC after the addition of the tracer.

117 *Bacterial Production*

118 Bacterial production was estimated from tritiated thymidine (^3H-Thymidine)
119 incorporation rates[26]. Briefly, 20 ml of water were incubated in gas tight serum bottles
120 with ^3H-Thy (ca. 80 Ci $mmol^{-1}$; ICN Pharmaceuticals) for two to four hours in the dark
121 at *in situ* temperature and at saturation conditions (ca. 50 nM of ^3H-Thy,[27]). After
122 incubation, cold trichloroacetic acid (TCA; 5.0%, fin. conc.) was added in order to stop
123 ^3H-Thy incorporation and samples were kept cold until passed through 0.22 μm pore-
124 size cellulose nitrate filters (Sartorius). Radioactivity associated with the filters was
125 estimated by liquid scintillation in a Liquid Scintillation Analyser Tri-Carb 2100TR
126 (Packard). Cell production was calculated from ^3H-Thy incorporation rates according to
127 recent calibrations[28].

128 *Fe-oxidation and reduction rate measurements.*

129 Water samples from selected depths corresponding to those with maximum of turbidity
130 and red fluorescence signals were incubated either *in situ* or *ex situ* for Fe-oxidation and
131 reduction rate measurements. *In situ* incubations were conducted by suspending
132 incubation vessels (25 ml glass syringes) at the depths of collection so the microbial
133 community experienced near *in situ* light conditions. Parallel vessels were incubated
134 under light and dark (aluminium foil for shielding) conditions, and changes in Fe-
135 speciation were monitored over time. Fe(II) accumulation rates in the dark syringes
136 were used to calculate Fe reduction rates, whereas the difference in Fe(II) accumulation
137 between light and dark syringes was used to calculate Fe oxidation rates. *Ex situ*

138 incubations were also conducted in glass syringes (100 ml) that were incubated under
139 15 μE m^{-2} s^{-1} of light (supplied by 60 W incandescent light bulb) with the addition of
140 DCMU (3-(3,4-dichlorophenyl)-1,1-dimethylurea or DCMU, 0.55 mg l^{-1}), a well-
141 known inhibitor of photosystem II and oxygenic photosynthesis[29,30]. Syringes were
142 subjected to alternating light and dark cycles. Rates of oxidation and reduction were
143 calculated from time course changes in Fe speciation[31,32].

144 *Sulfate reduction rates*

145 *In situ* sulfate reduction rates were determined using the ^{35}S radiotracer technique[33]

146 *Molecular analyses*

147 Water samples (0.5 to 1.0 l) for nucleic acid extraction were processed, filtered and
148 stored as previously described[34,35]. Genomic deoxyribonucleic acid (DNA) was
149 extracted from 0.22-μm filters and DNA extractions (*ca.* 50 μl at 60 – 250 ng μl^{-1}) from
150 each water depth were subsequently analysed by means of tag-encoded FLX-Titanium
151 amplicon pyrosequencing (TEFAP)[36,37] at Research and Testing Laboratory (Lubbock,
152 TX, USA). The archaeal and bacterial TEFAP (aTEFAP and bTEFAP, respectively)
153 were performed using previously described primers[37].

154 In order to obtain nearly full-length 16S rRNA gene sequences from pure cultures of
155 *Chlorobi* isolates from KB (see below), DNA was amplified with general bacterial
156 primers (27f – 1492r;[38,39]) and sequenced at external facilities.

157 *Pyrosequencing data analyses*

158 Pyrosequencing data was analysed using Mothur[40]. Briefly data was decompressed and
159 sequencing errors were reduced by trimming flows (i.e., denoising) and sequences by
160 applying the following quality criteria: amplicons shorter than 200 bp in length, reads
161 containing any unresolved nucleotides and more than 8 homopolimers were removed
162 from the archaeal and bacterial pyrosequencing-derived datasets. Subsequently,
163 improved sequences were processed from individual files. Putative chimeras (checked
164 by using Uchime software[41]) and contaminants (understood as those unclassified or
165 misclassified sequences) were removed from our sequence collection files. Afterwards,
166 alpha- and beta-diversity analyses by OTUs and phylogenetic relationships were
167 conducted. For the taxonomic adscription of both aTEFAP and bTEFAP amplicons, the

168 SEED alignment for archaea and bacteria from the SILVA databases was uploaded in
169 Mothur[40] and a confidence threshold of 80% (bootstrap) was applied. Relative
170 abundances of retrieved phylogenetic groups and hierarchical visualization was
171 performed with Krona tool version 2-4[42].

172 *Phylogenetic analyses of the GSB community present in KB*

173 bTEFAP sequences from KB water samples tentatively belonging to the *Chlorobi*
174 phylum and 16S rRNA gene sequences from KB isolates were subsequently analysed
175 for further taxonomic refinement. All sequences were aligned using the SINA aligner[43]
176 and then imported into the latest SILVA 16S rRNA-ARB-compatible database
177 (SSURef-111_NR_98_04_08_12_opt_v2.arb; http://www.arb-silva.de) in ARB[44]. Two
178 base frequency filters ("Termini" and "pos_var_ssuref:bacteria"; positional variability
179 by parsimony) were applied to exclude highly variable positions before adding
180 sequences to the original database using the "parsimony quick add marked" tool from
181 ARB. Sequence identities of representative OTUs retrieved from water samples with
182 respect to both *Chlorobium ferroooxidans* strain KoFox and KB isolates were
183 determined by pairwise comparisons in BLAST analyses[45].

184 *Culture conditions*

185 Water samples for culturing were collected from chemocline depths. Enrichment
186 cultures were initiated by supplementing lake water with a defined mineral media[46].
187 Isolates were obtained from these enrichment cultures through multiple serial dilutions.

188

189 **References of supplementary methods**

190 1. Damas, H. La stratification thermique et chimique des lacs Kivu, Édouard et
191 Ndalaga (Congo Belge). *Annales de la Société Royale Zoologique de Belgique*
192 **68,** 51–68 (1937).
193 2. Degens, E. T. & Kulbicki, G. Hydrothermal origin of metals in some East
194 African rift lakes. *Mineral Deposita* **8,** 388–404 (1973).
195 3. Degens, E. T., Herzen, R. P., Wong, H.-K., Deuser, W. G. & Jannasch, H. W.
196 Lake Kivu: structure, chemistry and biology of an East African rift lake. *Geol*
197 *Rundsch* **62,** 245–277 (1973).
198 4. Tietze, D. K. *et al.* The genesis of the methane in Lake Kivu (Central Africa).
199 *Geol Rundsch* **69,** 452–472 (1980).
200 5. Isumbisho, M., Sarmento, H., Kaningini, B., Micha, J.-C. & Descy, J.-P.
201 Zooplankton of Lake Kivu, East Africa, half a century after the Tanganyika
202 sardine introduction. *J Plankton Res* **28,** 971–989 (2006).
203 6. Sarmento, H., Isumbisho, M. & Descy, J.-P. Phytoplankton ecology of Lake
204 Kivu (eastern Africa). *J Plankton Res* **28,** 815–829 (2006).
205 7. Sarmento, H. *et al.* Abundance and distribution of picoplankton in tropical,
206 oligotrophic Lake Kivu, eastern Africa. *Freshwater Biol* **53,** 756–771 (2008).
207 8. Descy, J.-P., Darchambeau, F. & Schmid, M. *Lake Kivu*. 1–169 (Springer, 2012).
208 9. Borges, A. V. *et al.* Carbon cycling of Lake Kivu (East Africa): net autotrophy in
209 the epilimnion and emission of CO_2 to the atmosphere sustained by geogenic
210 inputs. *PLoS ONE* **9,** e109500 (2014).
211 10. Pasche, N., Dinkel, C., Müller, B., Schmid, M. & Wehrli, B. Physical and
212 biogeochemical limits to internal nutrient loading of meromictic Lake Kivu.
213 *Limnol. Oceanogr.* **54,** 1863–1873 (2009).
214 11. Schmid, M., Halbwachs, M., Wehrli, B. & Wüest, A. Weak mixing in Lake
215 Kivu: New insights indicate increasing risk of uncontrolled gas eruption.
216 *Geochem Geophys Geosyst* **6,** 1–11 (2005).
217 12. Viollier, E., Inglett, P. W., Hunter, K., Roychoudhury, A. N. & Van Cappellen,
218 P. The ferrozine method revisited: Fe(II)/Fe(III) determination in natural waters.
219 *Appl. Geochem.* **15,** 785–790 (2000).
220 13. Borges, A. V., Abril, G., Delille, B., Descy, J.-P. & Darchambeau, F. Diffusive
221 methane emissions to the atmosphere from Lake Kivu (Eastern Africa). *J.*
222 *Geophys. Res.* **116,** 1–15 (2011).
223 14. Weiss, R. F. Determinations of Carbon Dioxide and Methane by Dual Catalyst
224 Flame Ionization Chromatography and Nitrous Oxide by Electron Capture
225 Chromatography. *J Chromatogr Sci* **19,** 611–616 (1981).
226 15. Rice, E. W., Baird, R. B., Eaton, A. D. & Clesceri, L. S. *Standard Methods for*
227 *the Examination of Water Wastewater*. (2012).
228 16. Miranda, K. M., Espey, M. G. & Wink, D. A. A Rapid, Simple
229 Spectrophotometric Method for Simultaneous Detection of Nitrate and Nitrite.
230 *Nitric Oxide* **5,** 62–71 (2001).
231 17. Lovley, D. R. & Goodwin, S. Hydrogen concentrations as an indicator of the
232 predominant terminal electron-accepting reactions in aquatic sediments. *Geochim*
233 *Cosmochim Acta* **52,** 2993–3003 (1988).
234 18. Hoehler, T. M., Alperin, M. J., Albert, D. B. & Martens, C. S. Thermodynamic
235 control on hydrogen concentrations in anoxic sediments. *Geochim Cosmochim*
236 *Acta* **62,** 1745–1756 (1998).
237 19. Vandieken, V., Finke, N. & Thamdrup, B. Hydrogen, acetate, and lactate as

238 electron donors for microbial manganese reduction in a manganese-rich coastal
239 marine sediment. *FEMS Microbiology Ecology* **87,** 733–745 (2014).
240 20. Descy, J.-P., Higgins, H. W., Mackey, D. J., Hurley, J. P. & Frost, T. M. Pigment
241 ratios and phytoplankton assessment in northern Wisconsin lakes. *J. Phycol.* **36,**
242 274–286 (2000).
243 21. Wright, S. W. *et al.* Improved HPLC method for the analysis of chlorophylls and
244 carotenoids from marine phytoplankton. *Mar Ecol Prog Ser* **77,** 183–196 (1991).
245 22. Borrego, C. M. & Garcia-Gil, L. J. Separation of bacteriochlorophyll homologues
246 from green photosynthetic sulfur bacteria by reversed-phase HPLC. *Photosynth.*
247 *Res.* **41,** 157–164 (1994).
248 23. Borrego, C. M., Arellano, J. B., Abella Ametller, C. A., Gillbro, T. & Garcia-Gil,
249 J. The molar extinction coefficient of bacteriochlorophyll e and the pigment
250 stoichiometry in Chlorobium phaeobacteroides. *Photosynth. Res.* **60,** 257–264
251 (1999).
252 24. Sirevåg, R., Buchanan, B. B., Berry, J. A. & Troughton, J. H. Mechanisms of
253 CO2 fixation in bacterial photosynthesis studied by the carbon isotope
254 fractionation technique. *Arch. Microbiol.* **112,** 35–38 (1977).
255 25. Hama, T. *et al.* Measurement of photosynthetic production of a marine
256 phytoplankton population using a stable ^{13}C isotope. *Mar. Biol.* **73,** 31–36
257 (1983).
258 26. Fuhrman, J. A. & Azam, F. Thymidine incorporation as a measure of
259 heterotrophic bacterioplankton production in marine surface waters: Evaluation
260 and field results. *Mar. Biol.* **66,** 109–120 (1982).
261 27. Servais, P. Bacterioplanktonic biomass and production in the river Meuse
262 (Belgium). *Hydrobiologia* **174,** 99–110 (1989).
263 28. Stenuite, S. *et al.* Abundance and production of bacteria, and relationship to
264 phytoplankton production, in a large tropical lake (Lake Tanganyika).
265 *Freshwater Biol* **54,** 1300–1311 (2009).
266 29. Steenbergen, C. L. M. & van den Hoven, P. A note on the measurement of
267 production of phototrophic bacteria in deep layers. *Arch. Hydrobiol. Beih.*
268 *Ergebn. Limnol.* **34,** 349–355 (1990).
269 30. Jørgensen, B. B., Kuenen, J. G. & Cohen, Y. Microbial transformations of sulfur
270 compounds in a stratified lake (Solar Lake, Sinai). *Limnol. Oceanogr.* **24,** 799–
271 822 (1979).
272 31. Crowe, S. A. *et al.* Photoferrotrophs thrive in an Archean Ocean analogue. *Proc.*
273 *Natl. Acad. Sci. USA* **105,** 15938–15943 (2008).
274 32. Crowe, S. A. *et al.* The methane cycle in ferruginous Lake Matano. *Geobiology*
275 **9,** 61–78 (2011).
276 33. Fossing, H. & Jørgensen, B. B. Measurement of bacterial sulfate reduction in
277 sediments – Evaluation of a single-step Chromium reduction method.
278 *Biogeochemistry* **8,** 205–222 (1989).
279 34. Llirós, M. *et al.* Vertical distribution of ammonia-oxidizing crenarchaeota and
280 methanogens in the epipelagic waters of Lake Kivu (Rwanda-Democratic
281 Republic of the Congo). *Appl Environ Microbiol* **76,** 6853–6863 (2010).
282 35. Llirós, M., Casamayor, E. O. & Borrego, C. M. High archaeal richness in the
283 water column of a freshwater sulfurous karstic lake along an interannual study.
284 **66,** 331–342 (2008).
285 36. Dowd, S. E. *et al.* Evaluation of the bacterial diversity in the feces of cattle using
286 16S rDNA bacterial tag-encoded FLX amplicon pyrosequencing (bTEFAP).
287 *BMC Microbiol* **8,** 125 (2008).

288 37. Shah, V. *et al.* Bacterial and archaea community present in the Pine Barrens
289 Forest of Long Island, NY: unusually high percentage of ammonia oxidizing
290 bacteria. *PLoS ONE* **6,** e26263 (2011).
291 38. Suzuki, M. & Giovannoni, S. J. Bias Caused by Template Annealing in the
292 Amplification of Mixtures of 16S rRNA Genes by PCR. *Appl Environ Microbiol*
293 **62,** 625–630 (1996).
294 39. Stahl, D. A. & Amann, R. in *Nucleic Acid Techniques in Bacterial Systematics*
295 (eds. Stackebrandt, E. & Goodfellow, M.) 205–248 (John Wiley & Sons, Inc.,
296 1991).
297 40. Schloss, P. D. *et al.* Introducing mothur: open-source, platform-independent,
298 community-supported software for describing and comparing microbial
299 communities. *Appl Environ Microbiol* **75,** 7537–7541 (2009).
300 41. Edgar, R. C., Haas, B. J., Clemente, J. C., Quince, C. & Knight, R. UCHIME
301 improves sensitivity and speed of chimera detection. *Bioinformatics* **27,** 2194–
302 2200 (2011).
303 42. Ondov, B. D., Bergman, N. H. & Phillippy, A. M. Interactive metagenomic
304 visualization in a Web browser. *BMC Bioinformatics* **12,** 385 (2011).
305 43. Pruesse, E., Peplies, J. & Glöckner, F. O. SINA: accurate high-throughput
306 multiple sequence alignment of ribosomal RNA genes. *Bioinformatics* **28,** 1823–
307 1829 (2012).
308 44. Ludwig, W. *et al.* ARB: a software environment for sequence data. *Nucleic Acids*
309 *Res.* **32,** 1363–1371 (2004).
310 45. Altschul, S. F., Gish, W., Miller, W., Myers, E. W. & Lipman, D. J. Basic local
311 alignment search tool. *J Mol Biol* **215,** 403–410 (1990).
312 46. Hegler, F., Posth, N. R., Jiang, J. & Kappler, A. Physiology of phototrophic
313 iron(II)-oxidizing bacteria: implications for modern and ancient environments.
314 **66,** 250–260 (2008).
315
316

317 *Captions to Supplementary Figures*

318 **Supplementary Figure S1. Sample location map.** Map showing the location of
319 Kabuno Bay, Sake river and hydrothermal spring sampling sites (red dots). Maps were
320 generated by hand-drawing using Adobe Illustrator® software.

321 **Supplementary Figure S2. Kabuno Bay vertical profiles.** Data in the upper panels are
322 from the rainy season (RS; February 2012) and lower panels from the dry season (DS;
323 October 2012). **a** and **c**: CH_4 (light blue square), H_2 (grey dots), NO_x (*i.e.*, $NO_2^- + NO_3^-$)
324 (yellow dots) and CH_3COO^- (white squares) concentrations; **b** and **f**: relative abundance
325 of bacterial OTUs grouped by putative activity (i.e., oxygenic phototrophs (Ox PhS,
326 brown dots), anoxygenic phototrophs (Anox PhS (GSB), light green dots), Fe or Mn
327 related bacterial OTUs (red triangles)); **c** and **g**: relative abundance of archaeal OTUs
328 grouped by putative activity (i.e., ammonia oxidizing Archaea (AOA, yellow triangles),
329 acetoclastic methanogens (light blue diamonds) and hydrogenotrophic methanogens
330 (light blue dots)); **d**: ^{3}H-Thymidine uptake (nM ^{3}H-Thymidine h^{-1}, white triangles).

331 **Supplementary Figure S3. *Chlorobi* and related groups diversity.** Collapsed 16S
332 rRNA gene phylogenetic tree of the *Chlorobi* and related groups members detected in
333 KB (grey shadow). The number of sequences assigned to each phylogenetic clade and
334 the relative abundance (pie charts) of the retrieved sequences in each clade is indicated.
335 The tree includes sequences retrieved by pyrosequencing from all depths and seasons
336 (RS and DS), and also full 16S rRNA gene sequences from our KB pure culture. Pie
337 charts depict the OTUs retrieved from each water compartment (E stands for
338 epilimnion, C for chemocline and M for monimolimnion) and size is proportional to the
339 number of sequences (log transformed) from the OTUs ascribed to each cluster. The
340 scale bar indicates 0.10 fixed point mutation per nucleotide position.

341 **Supplementary Figure S4. Kabuno Bay GSB sequence similarities.** Box plots
342 summarizing sequence identities of representative KB OTUs with respect to both *Chl.*
343 *ferrooxidans* str. KoFox and to KB isolate.

344 **Supplementary Figure S5. Pigment analyses.** Example of a HPLC chromatogram
345 from a natural KB water sample (10.6 m depth, DS) showing the main BChl *e*
346 homologues (farnesyl esterified), the secondary homologues (non-farnesyl esterified)
347 and carotenoids (mainly isorenieratene and ß-isorenieratene).

348 **Supplementary Figure S6. Fe oxidation rates from Kabuno Bay isolate.** Fe(II)
349 oxidation rates for KB isolate incubated under high (black diamonds, 14.5 μE m^{-2} s^{-1})
350 and low (grey diamonds, 0.64 μE m^{-2} s^{-1}) light intensities.

351

Supplementary table 1. **Physico-chemical characteristics of Kabuno Bay and surrounding water inputs.** Comparison of main physico-chemical parameters measured in the Sake river and hydrothermal spring near Sake Bay in comparison to KB.

	Kabuno Bay			**Sake River**	**Hydrothermal spring**
GPS coordinates	1º37.252' S, 29º2.976' E			1°34.078' S, 29°3.236' E	1°33.744' S, 29°2.836' E
Depth (m)	Chemocline 10.5 – 11.5	65.0	Deep waters 100.0	Surface 0.1	Surface 0.1
Altitude (m.a.s.l.)	1,463	1,463	1,463	1,515	1,485
Temperature (ºC)	22.96	24.07	24.78	18.55	29.45
pH	6.25	6.1	6.1	6.05	6.32
Dissolved oxygen (mg l^{-1})	2.5	0.0	0.0	1.9	0
Conductivity (mS cm^{-1})	3.27	6.58	7.48	1.29	5.20
Cl^- (mM)	Na[a]	2.1	Na	Na	15.3
SO_4^{2-} (µM)	485,61	0.7	Na	Na	1,574
Fe (II) (µM)	289,79	689	422	0	410

[a]Na, not analysed.

Sup Table 2 - Taxonomic afiliations Kabuno Bay

				February 2012												October 2012										
Domain	**Phylum**	**Class**	**Order**	**total seqs**	**1**	**4**	**10**	**10.5**	**10.75**	**11**	**11.25**	**11.5**	**12**	**15**	**30**	**total seqs**	**1**	**6**	**9**	**9.5**	**10**	**10.3**	**10.6**	**11.1**	**15**	**30**
k__Bacteria	p__Actinobacteria			775	215	356	92	12	3	8	9	16	17	45	2	2401	450	331	354	532	424	8	103	112	85	2
k__Bacteria	p__Armatimonadetes			112	0	5	2	3	6	5	14	12	33	22	10	68	1	1	4	5	2	0	1	54	0	0
k__Bacteria	p__Bacteroidetes			861	54	81	52	48	61	51	85	115	103	137	74	1149	170	86	71	131	173	1	73	418	23	3
k__Bacteria	p__Bacteroidetes	c__Bacteroidia		15	0	0	5	3	0	0	2	1	0	3	1	27	0	0	0	0	0	0	16	11	0	0
k__Bacteria	p__Bacteroidetes	c__Flavobacteria		35	9	10	7	0	0	0	3	1	1	3	1	145	26	5	19	29	59	0	5	2	0	0
k__Bacteria	p__Bacteroidetes	c__Sphingobacteria		152	25	41	11	4	4	5	10	18	10	19	5	400	97	50	32	69	49	1	27	59	14	2
k__Bacteria	p__Bacteroidetes	unclassified		659	20	30	29	41	57	46	70	95	92	112	67	577	47	31	20	33	65	0	25	346	9	1
k__Bacteria	p__Chlorobi			1916	8	8	108	265	326	320	229	208	109	183	152	811	23	15	29	42	52	0	122	528	0	0
k__Bacteria	p__Chlorobi	c__Chlorobia		1462	0	1	81	225	274	263	170	143	60	125	120	575	1	0	14	17	26	0	107	410	0	0
k__Bacteria	p__Chlorobi	c__Ignavibacteria		356	0	0	23	35	41	47	44	56	40	43	27	123	0	0	2	4	2	0	15	100	0	0
k__Bacteria	p__Chlorobi	c__OPB56		39	8	7	4	0	0	2	5	4	5	3	1	102	22	15	13	21	24	0	0	7	0	0
k__Bacteria	p__Chlorobi	unclassified		59	0	0	0	5	11	8	10	5	4	12	4	11	0	0	0	0	0	0	0	11	0	0
k__Bacteria	p__Chloroflexi			824	9	13	26	64	33	60	83	88	132	251	65	444	49	29	22	30	83	0	7	224	0	0
k__Bacteria	p__Cyanobacteria			910	243	337	59	19	25	20	18	24	60	48	57	1052	223	168	126	205	164	0	67	97	2	0
k__Bacteria	p__Firmicutes			46	2	2	1	0	3	0	0	3	2	2	31	341	4	5	7	11	0	126	76	20	49	43
k__Bacteria	p__Nitrospirae			102	0	0	3	5	5	6	17	29	10	11	16	29	0	0	0	1	3	0	0	25	0	0
k__Bacteria	p__Planctomycetes			136	33	32	10	3	3	1	7	9	23	2	13	360	134	32	35	54	50	0	14	41	0	0
k__Bacteria	p__Proteobacteria			2945	176	272	601	214	200	128	205	241	231	384	293	5259	646	424	438	759	941	87	671	1115	97	81
k__Bacteria	p__Proteobacteria	c__Alphaproteobacteria		501	92	136	48	28	38	21	27	23	22	42	24	1623	346	221	190	349	269	7	117	114	10	0
k__Bacteria	p__Proteobacteria	c__Alphaproteobacteria	o__Caulobacterales	15	2	1	3	1	0	0	0	1	5	1	1	123	11	10	15	28	5	0	20	34	0	0
k__Bacteria	p__Proteobacteria	c__Alphaproteobacteria	o__Rhizobiales	16	3	3	2	1	0	2	3	1	0	1	0	54	6	0	4	14	2	1	8	19	0	0
k__Bacteria	p__Proteobacteria	c__Alphaproteobacteria	o__Rhodobacterales	143	5	3	6	22	32	16	15	14	4	11	15	76	6	1	0	14	16	6	18	5	10	0
k__Bacteria	p__Proteobacteria	c__Alphaproteobacteria	o__Rhodospirillales	62	6	12	8	3	3	2	4	1	3	16	4	113	14	11	12	18	29	0	13	16	0	0
k__Bacteria	p__Proteobacteria	c__Alphaproteobacteria	o__Rickettsiales	220	73	109	16	0	1	0	3	2	5	10	1	1034	276	186	140	211	181	0	35	5	0	0
k__Bacteria	p__Proteobacteria	c__Alphaproteobacteria	o__Sphingomonadales	18	0	0	7	1	0	0	1	2	4	0	3	100	5	4	2	33	3	0	22	31	0	0
k__Bacteria	p__Proteobacteria	c__Alphaproteobacteria	unclassified	27	3	8	6	0	2	1	1	2	1	3	0	123	28	9	17	31	33	0	1	4	0	0
k__Bacteria	p__Proteobacteria	c__Betaproteobacteria		1294	57	86	268	139	136	85	84	75	47	103	214	1550	137	85	117	194	337	65	286	268	40	21
k__Bacteria	p__Proteobacteria	c__Betaproteobacteria	o__Burkholderiales	706	22	42	142	93	61	43	39	39	28	45	152	865	65	47	48	100	153	62	179	150	40	21
k__Bacteria	p__Proteobacteria	c__Betaproteobacteria	o__Gallionellales	50	0	0	26	8	0	0	0	0	2	14	0	135	0	1	6	11	50	0	31	36	0	0
k__Bacteria	p__Proteobacteria	c__Betaproteobacteria	o__Hydrogenophilales	0	0	0	0	0	0	0	0	0	0	0	0	1	0	0	0	0	0	1	0	0	0	0
k__Bacteria	p__Proteobacteria	c__Betaproteobacteria	o__Methylophilales	71	6	8	44	2	2	0	1	0	1	7	0	177	17	6	21	26	69	0	28	10	0	0
k__Bacteria	p__Proteobacteria	c__Betaproteobacteria	o__Neisseriales	1	0	0	0	0	0	0	0	1	0	0	0	0	0	0	0	0	0	0	0	0	0	0
k__Bacteria	p__Proteobacteria	c__Betaproteobacteria	o__Rhodocyclales	109	0	0	23	12	8	10	13	8	7	17	11	87	0	0	5	6	25	1	17	33	0	0
k__Bacteria	p__Proteobacteria	c__Betaproteobacteria	unclassified	357	29	36	33	24	65	32	31	27	9	20	51	285	55	31	37	51	40	1	31	39	0	0
k__Bacteria	p__Proteobacteria	c__Deltaproteobacteria		471	7	5	12	13	15	14	29	70	92	180	34	541	14	12	19	29	47	0	16	404	0	0
k__Bacteria	p__Proteobacteria	c__Deltaproteobacteria	o__Bdellovibrionales	1	0	0	0	0	0	0	0	1	0	0	0	8	3	2	0	3	0	0	0	0	0	0
k__Bacteria	p__Proteobacteria	c__Deltaproteobacteria	o__Desulfobacterales	5	0	0	0	0	0	0	1	0	4	0	0	12	0	0	0	0	0	0	1	11	0	0
k__Bacteria	p__Proteobacteria	c__Deltaproteobacteria	o__Desulfuromonadales	12	0	1	5	0	0	0	0	1	1	4	0	22	0	0	0	4	7	0	6	5	0	0
k__Bacteria	p__Proteobacteria	c__Deltaproteobacteria	o__MIZ46	13	5	4	3	0	1	0	0	0	0	0	0	44	9	7	16	11	1	0	0	0	0	0
k__Bacteria	p__Proteobacteria	c__Deltaproteobacteria	o__Myxococcales	6	2	0	3	0	1	0	0	0	0	0	0	53	2	1	2	7	29	0	0	12	0	0
k__Bacteria	p__Proteobacteria	c__Deltaproteobacteria	o__Syntrophobacterales	371	0	0	0	9	12	14	26	58	78	150	24	314	0	0	1	2	7	0	5	299	0	0
k__Bacteria	p__Proteobacteria	c__Deltaproteobacteria	unclassified	63	0	0	1	4	1	0	2	10	9	26	10	88	0	2	0	2	3	0	4	77	0	0
k__Bacteria	p__Proteobacteria	c__Epsilonproteobacteria		17	0	0	1	0	0	0	0	2	2	12	0	98	0	0	0	3	2	0	52	41	0	0
k__Bacteria	p__Proteobacteria	c__Epsilonproteobacteria	o__Campylobacterales	17	0	0	1	0	0	0	0	2	2	12	0	98	0	0	0	3	2	0	52	41	0	0
k__Bacteria	p__Proteobacteria	c__Gammaproteobacteria		545	15	26	229	29	7	6	61	65	58	31	18	1238	118	86	90	148	229	15	188	257	47	60
k__Bacteria	p__Proteobacteria	c__Gammaproteobacteria	o__Aeromonadales	2	0	2	0	0	0	0	0	0	0	0	0	1	1	0	0	0	0	0	0	0	0	0
k__Bacteria	p__Proteobacteria	c__Gammaproteobacteria	o__Alteromonadales	12	3	1	0	0	0	0	3	3	2	0	0	42	11	5	2	1	2	0	18	3	0	0
k__Bacteria	p__Proteobacteria	c__Gammaproteobacteria	o__Chromatiales	33	5	12	4	1	2	0	1	0	5	1	2	72	14	19	14	18	4	0	0	3	0	0
k__Bacteria	p__Proteobacteria	c__Gammaproteobacteria	o__Legionellales	14	0	1	2	0	2	1	1	0	1	1	5	56	11	3	6	17	10	0	0	9	0	0
k__Bacteria	p__Proteobacteria	c__Gammaproteobacteria	o__Methylococcales	42	0	0	19	5	1	0	0	4	1	12	0	67	0	0	5	3	35	0	9	15	0	0
k__Bacteria	p__Proteobacteria	c__Gammaproteobacteria	o__Oceanospirillales	1	1	0	0	0	0	0	0	0	0	0	0	4	0	0	3	0	0	1	0	0	0	0
k__Bacteria	p__Proteobacteria	c__Gammaproteobacteria	o__Pasteurellales	0	0	0	0	0	0	0	0	0	0	0	0	9	0	0	0	0	0	0	2	0	0	7
k__Bacteria	p__Proteobacteria	c__Gammaproteobacteria	o__Pseudomonadales	191	1	3	24	7	0	3	52	53	41	1	6	636	63	53	53	82	56	0	83	158	40	48
k__Bacteria	p__Proteobacteria	c__Gammaproteobacteria	o__Xanthomonadales	11	0	0	3	1	0	2	0	1	0	0	4	81	0	0	0	7	1	5	41	15	7	5
k__Bacteria	p__Proteobacteria	c__Gammaproteobacteria	unclassified	239	5	7	177	15	2	0	4	4	8	16	1	270	18	6	7	20	121	9	35	54	0	0
k__Bacteria	p__Proteobacteria	unclassified	unclassified	117	5	19	43	5	4	2	4	6	10	16	3	209	31	20	22	36	57	0	12	31	0	0
k__Bacteria	p__Spirochaetes			45	0	1	0	0	1	0	4	7	14	17	1	75	0	0	0	0	1	0	2	71	0	1
k__Bacteria	p__Verrucomicrobia			80	14	20	11	2	3	0	3	5	5	13	4	239	41	10	30	60	31	0	24	43	0	0
k__Bacteria	other Cult phyla			55	2	6	3	4	1	1	4	7	5	10	12	73	5	2	5	7	3	0	3	30	0	18
k__Bacteria	Cand. Uncult phyla			301	0	0	9	15	22	26	50	59	62	38	20	327	10	4	13	25	42	0	41	192	0	0
k__Bacteria	unclassified			2967	63	126	95	164	177	214	295	468	467	661	237	2924	273	93	111	247	309	1	105	1785	0	0

1 **Supplementary table 3**. **Microbial richness and diversity in Kabuno Bay.**
2 Archaeal and bacterial richness and diversity estimates based on pyrosequencing
3 analyses from rainy (RS) and dry (DS) seasons in KB.
4
5

Water compartment	# OTUs	Coverage	Richness Chao1	Diversity Shannon
February – RS				
Archaea				
Epilimnion	12	0.99	17	0.3
Chemocline	45	0.99	88	0.7
Monimolimnion	48	0.99	57	1.4
Bacteria				
Epilimnion	776	0.85	1,825	5.4
Chemocline	1,095	0.86	2,837	5.3
Monimolimnion	1,225	0.82	2,859	6.2
October – DS				
Archaea				
Epilimnion	2	–	3	0.7
Chemocline	33	0.98	57	1.5
Monimolimnion	8	0.99	10	0.6
Bacteria				
Epilimnion	109	0.90	2,674	5.2
Chemocline	1,917	0.87	4,784	6.4
Monimolimnion	56	0.94	106	3.3

6
7
8

Spring

River

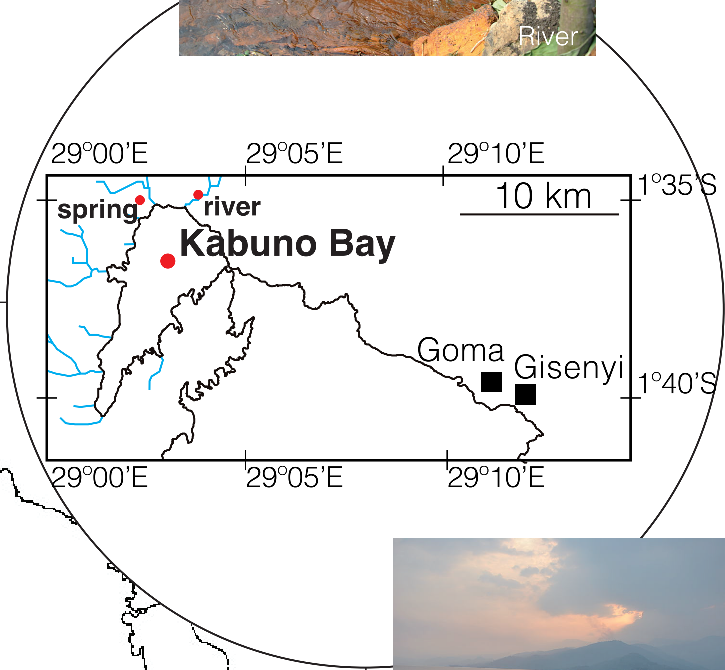
29°00'E
29°05'E
29°10'E
1°35'S
10 km
spring
river
Kabuno Bay
Goma
Gisenyi
1°40'S
29°00'E
29°05'E
29°10'E

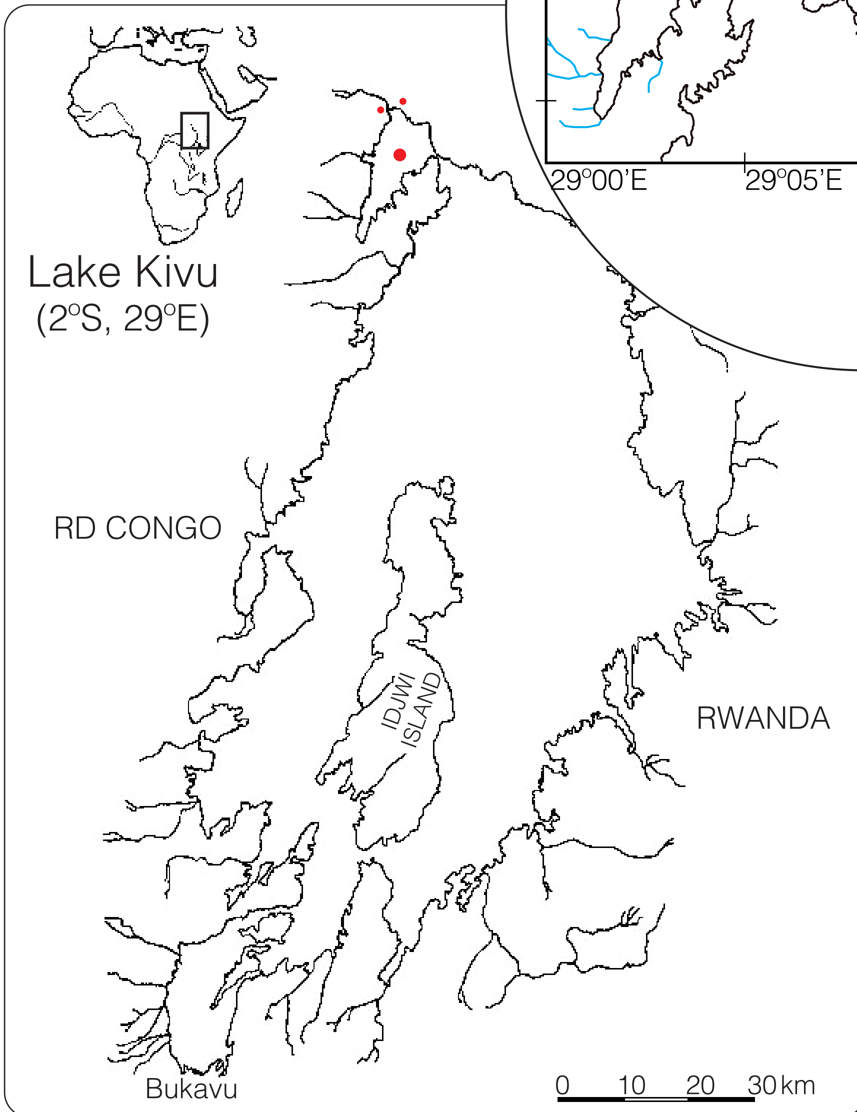
Lake Kivu
(2°S, 29°E)
RD CONGO
IDJWI ISLAND
RWANDA
Bukavu
0 10 20 30 km

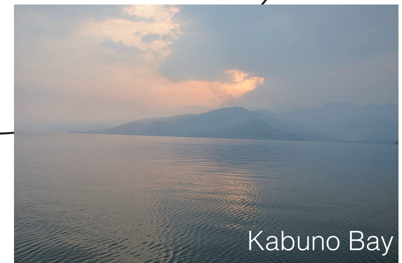
Kabuno Bay

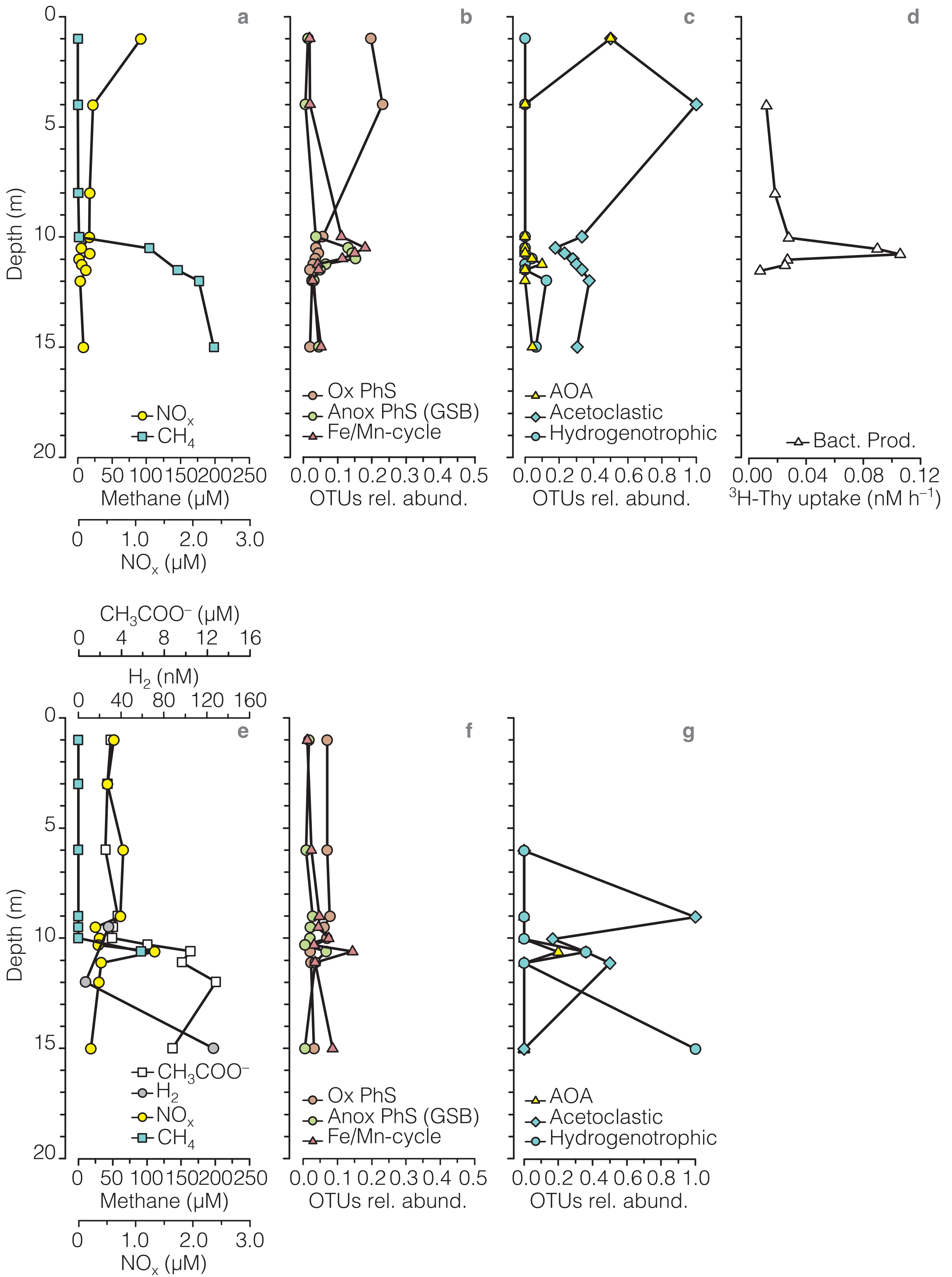

a
b
c
d
e
f
g
Depth (m)
NOx
CH4
Ox PhS
Anox PhS (GSB)
Fe/Mn-cycle
AOA
Acetoclastic
Hydrogenotrophic
Bact. Prod.
Methane (µM)
NOx (µM)
OTUs rel. abund.
3H-Thy uptake (nM h−1)
CH3COO− (µM)
H2 (nM)
CH3COO−
H2

RS
DS
Bacteroides
fragilis NCTC 9343,
CR626927
C 65%
E 6%
M 31%
E 4%
C 97%
155
Chlorobium_2
(*Chl. ferroxidans* cluster therein)
19
Chlorobium_1
C 100 %
3 Prosthecochloris_1
4 Prosthecochloris_2
7 Prosthecochloris_3
2 Prosthecochloris_4
FJ716306, Chlorobiaceae, Unl0b079
5
uncultured
FJ716275, Chlorobiaceae, Unl0b03x
3 Prosthecochloris_5
AJ428427, Chlorobiaceae, UnlCh811
2 uncultured
RS
DS
E 58%
M 16%
C 27%
C 100%
39
Chlorobaculum
2 Chlorobium_6
EF153291, Chlorobiaceae, ChrSpec5
HQ602908, Chlorobiaceae, Unl0zo8c
FJ716288, Chlorobiaceae, Unl0b06u
18 uncultured
FJ628275, Chlorobiaceae, Unl0aiev
3 Chloroherpeton
11 uncultured
5 uncultured
61 SJA–28
191
OPB56 (3 subclusters therein)
C 100%
C 100%
E 100%
E 79%
C 22%
E 50%
M 50%
Chlorobia - Chlorobiales
Chlorobiaceae
C 49%
E 13%
M 39%
E 20%
C 80%
66
PHOS–HE36 (3 subclusters therein)
51
Ignavibacteriaceae_Ignavibacterium
C 50%
M 50%
C 100%
5 LD–RB–34
AB486936, Ignavibacteria_Ignavibacteriales, Unl23731
C 41%
E 7%
M 53%
C 100%
19 **SR–FBR–L83**
31 **BSV40**
E 20%
C 80%
C 100%
49 **IheB3–7**
AJ347765, Ignavibacteria_Ignavibacteriales, UnltrSB2
FR667819, Ignavibacteria_Ignavibacteriales, Unl0d7ea
3 SM1H02
C 39%
M 62%
C 100%
104 BSV26
C 60%
M 40%
C 100%
Ignavibacteria - Ignavibacteriales
0.1

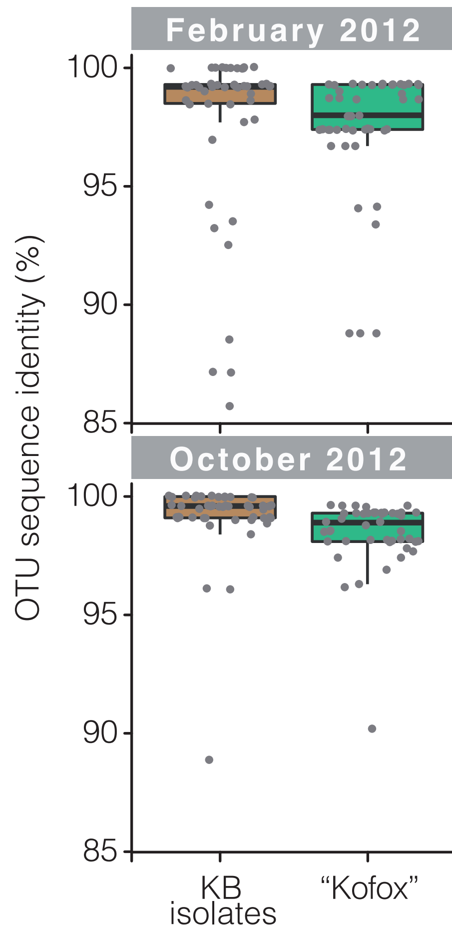
February 2012
October 2012
OTU sequence identity (%)
100
95
90
85
KB
isolates
“Kofox”

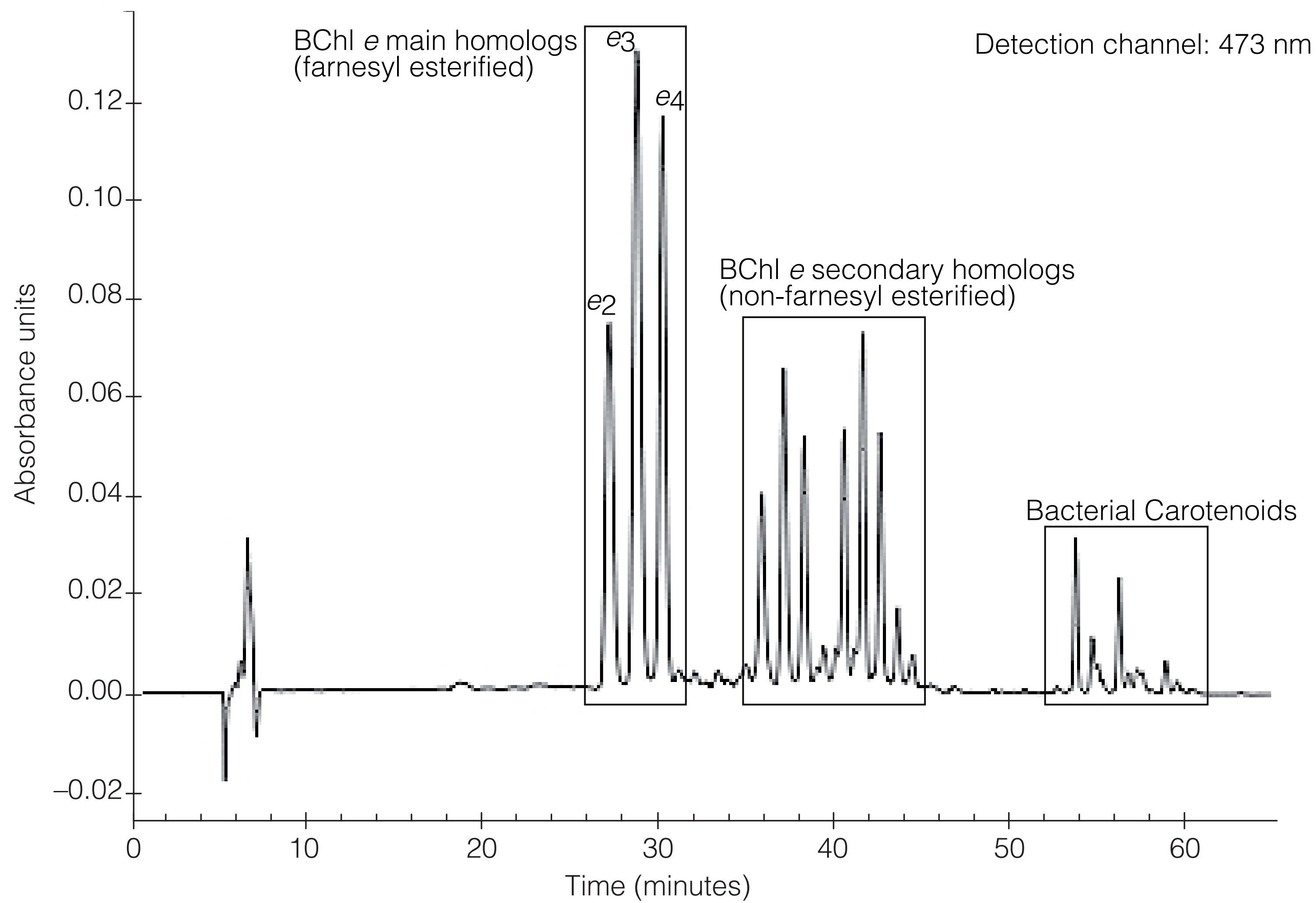

BChl *e* main homologs
(farnesyl esterified)
*e*3
*e*4
*e*2
Detection channel: 473 nm
BChl *e* secondary homologs
(non-farnesyl esterified)
Bacterial Carotenoids
Absorbance units
0.12
0.10
0.08
0.06
0.04
0.02
0.00
–0.02
0
10
20
30
40
50
60
Time (minutes)

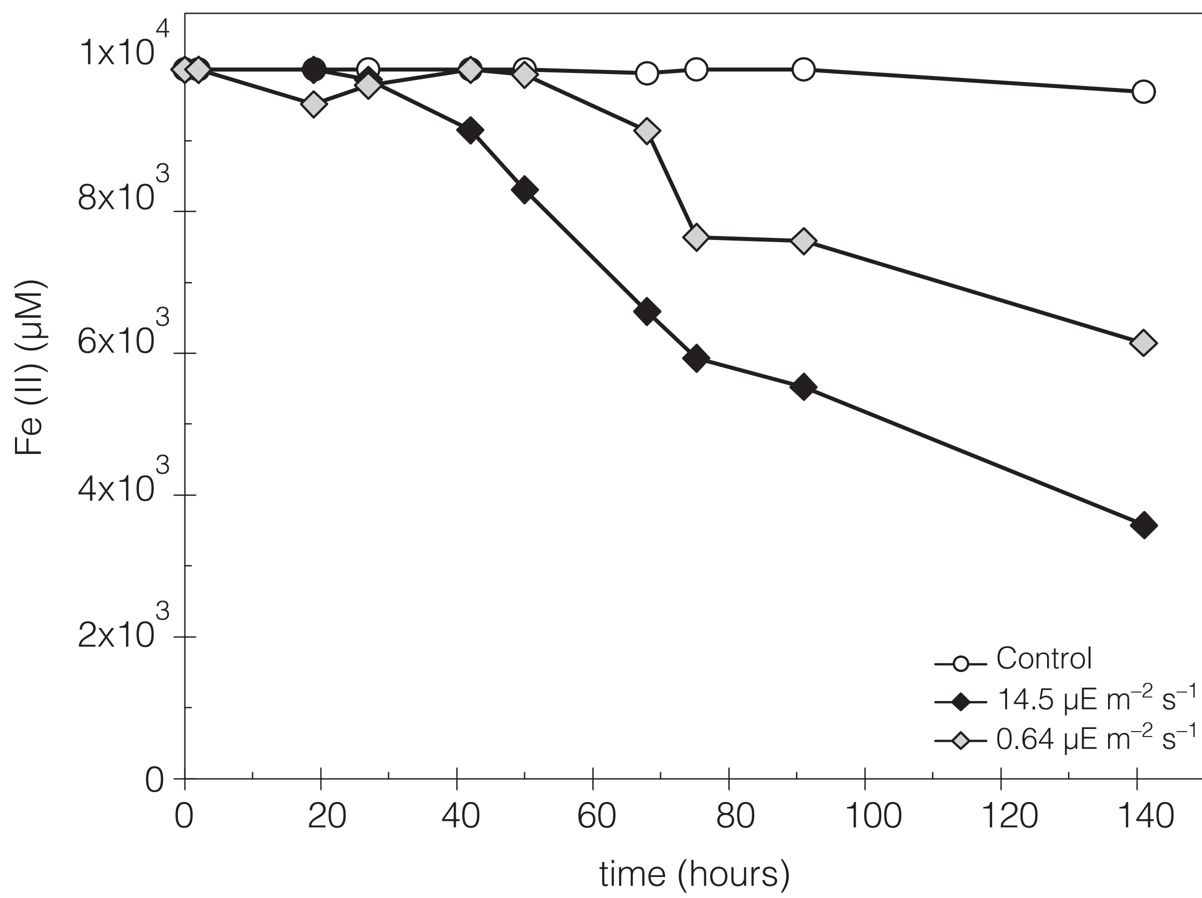

Fe (II) (μM)
1x10^4
8x10^3
6x10^3
4x10^3
2x10^3
0
0
20
40
60
80
100
120
140
time (hours)
Control
14.5 μE m^-2 s^-1
0.64 μE m^-2 s^-1